NJC

Accepted Manuscript

This is an *Accepted Manuscript*, which has been through the Royal Society of Chemistry peer review process and has been accepted for publication.

Accepted Manuscripts are published online shortly after acceptance, before technical editing, formatting and proof reading. Using this free service, authors can make their results available to the community, in citable form, before we publish the edited article. We will replace this *Accepted Manuscript* with the edited and formatted *Advance Article* as soon as it is available.

You can find more information about *Accepted Manuscripts* in the Information for Authors.

Please note that technical editing may introduce minor changes to the text and/or graphics, which may alter content. The journal's standard Terms & Conditions and the Ethical guidelines still apply. In no event shall the Royal Society of Chemistry be held responsible for any errors or omissions in this *Accepted Manuscript* or any consequences arising from the use of any information it contains.

ROYAL SOCIETY OF CHEMISTRY

www.rsc.org/njc

Two potential self-activated orthoborates $Cd_4NdO(BO_3)_3$ and $Ca_3Nd_3(BO_3)_5$: Growth, crystal structures and optical properties

Xing Wang[a,b], Mingjun Xia[a] and R. K. Li[*a]

Two neodymium orthoborate crystals of $Cd_4NdO(BO_3)_3$ and $Ca_3Nd_3(BO_3)_5$ were successfully grown by the flux method. Single crystal X-ray diffraction exhibits that $Cd_4NdO(BO_3)_3$ crystallizes in the monoclinic space group of *C*m with unit cell parameters a = 8.0536(14) Å, b = 15.872(2) Å, c = 3.5364(6) Å, β = 100.268(7)° and $Ca_3Nd_3(BO_3)_5$ has a hexagonal space group of $P6_3mc$ with cell parameters a = 10.4864(2) Å, c = 6.2665(1) Å. Both compounds have high Nd^{3+} concentration with 4.5×10^{21} ions/cm^3 in $Cd_4NdO(BO_3)_3$ and 1.0×10^{22} ions/cm^3 in $Ca_3Nd_3(BO_3)_5$, respectively. The absorption and emission spectra as well as decay curves for the $^4F_{3/2}$ to $^4I_{11/2}$ transition of Nd^{3+} ions in the two compounds were measured at room temperature. The spectra indicate that both two crystals are potential materials as self-activated microchip laser media due to high Nd^{3+} contents.

Introduction

Microchip lasers have been of continuing interest for their capabilities that exceed those of conventional lasers due to low cost, extremely compact and potentially mass producible characteristics. Furthermore, their outstanding potential advantages also include single-frequency output, high rates of frequency modulation and short-pulsed operation, and high power output by passive Q switching. [1] To fabricate microchip lasers, high gain media with small dimensions is required so that the activator (usually Nd^{3+}) concentrations in gain materials should be as high as possible. [2, 3] However, high dopant concentrations can cause a drastic decrease in the laser efficiency because of the so-called concentration quenching effect. [4] For instance, in most host materials with high neodymium-content, some physical properties such as fluorescence lifetime and optical quality are undesirably affected due to the existence of concentration quenching. [5] Therefore, microchip lasers with self-activated crystals [6] such as $NdAl_3(BO_3)_4$ (NAB) [4], $NdNa_5(WO_4)_4$ [7], and NdP_5O_{14} [8], have been realized in materials with Nd^{3+} ions occupying unique crystalline lattice sites and the uniformity of activators can contribute to enhance the optical quality of the laser element. Among above mentioned self-activated crystals, NAB is the most attractive, and recently watt-level continuous wave [9] and short pulse duration [5] microchip lasers have been reported. Nevertheless, the decay time of $^4F_{3/2}$ to $^4I_{11/2}$ transition in NAB is about 20 μs, which is much shorter than that of commercial Nd: YAG laser (230 μs), and it is still difficult to grow NAB crystals with sufficient size and high optical quality [10], thus it is very necessary to explore new self-activated materials, especially with high activator content.

Two series of rare earth borates, $Ca_3La_3(BO_3)$ [11, 12] and $Cd_4ReO(BO_3)_3$ (Re=Y, Gd, Lu) [13] were previously reported. Based on the structures of the compounds, the concentrations of the rare earth elements can be calculated as about 1×10^{22} ions/cm^3 for $Ca_3La_3(BO_3)$ and about 4.5×10^{21} ions/cm^3 for $Cd_4ReO(BO_3)_3$. Therefore the study of the Nd-analogs of the two compounds is worthwhile for their high concentrations of the rare-earth elements. In this paper, we present crystal growth, structures and luminescent properties of the Nd-counterpart borates and assess their possibilities in utilizing as self-activated laser crystals.

Experimental Section

Solid state syntheses and single-crystal growth

Polycrystalline samples of $Cd_4NdO(BO_3)_3$ were synthesized with the raw materials of CdO, Nd_2O_3, H_3BO_3 in stoichiometric ratio. The mixtures were first preheated at 500 °C for five hours and then calcined at 950 °C for 24 h with several intermediate grindings. The purity of the synthesized samples was checked by X-ray powder diffraction (XRD) at room temperature on a Bruker D8 diffractometer with Cu Ka radiation with scanning step and rate of 0.02 ° and 0.05 s/step in the 2θ range from 7 to 70°. However, it is unsuccessful to synthesize the $Ca_3Nd_3(BO_3)_5$ pure samples with several runs by the similar solid-state reaction route at different temperatures. The main phase of X-ray diffraction patterns is identified as $NdBO_3$.

$Cd_4NdO(BO_3)_3$ and $Ca_3Nd_3(BO_3)_5$ crystals were both grown by spontaneous crystallization with corresponding fluxes. In the growth process of crystal $Cd_4NdO(BO_3)_3$, analytical pure chemicals with the molar ratio of $CdO/Nd_2O_3/H_3BO_3$/ NaF = 4:0.5:3:1 were weighed and mixed thoroughly. The mixtures were put in a platinum crucible and heated up to 950 °C, held for 12 h for completely melting and homogenizing, then cooled to 800 °C at a rate of 5 °C /h, and finally cooled to room temperature. Violet crystalline grains could be found on the surface of solidified melt in the crucible and the crystals were mechanically separated from the matrix. The growth of $Ca_3Nd_3(BO_3)_5$ crystals experienced the similar process with an molar ratio of $CaCO_3/Nd_2O_3/H_3BO_3$/LiF = 3:1.5:5:8,

among which 8 molar LiF were served as flux to lower the crystallization temperature. After ground thoroughly, the materials were heated up to 750 °C and maintained for 12 h, then cooled at a rate of 5 °C/ h to 680 °C, and finally followed by natural cooling to room temperature. The violet crystal needles were chosen for single-crystal measurements.

Structures determination

Two pieces of violet crystals, $Cd_4NdO(BO_3)_3$ with dimensions of 0.12 × 0.07 × 0.04 mm^3 and $Ca_3Nd_3(BO_3)_5$ with dimensions of 0.13 × 0.11 × 0.10 mm^3, were selected for structure determination. The crystal data were collected on a Rigaku XtaLAB mini single-crystal X-ray diffractometer equipped with MoKα radiation (λ = 0.71073 Å) at room temperature. The crystal structures were solved with SHELXS-2014 by the direct method and refined with SHELXL-2014 program [14], which gave the final agreement indices of R_1=0.0320 and wR_2=0.0745 in $Cd_4NdO(BO_3)_3$ and R_1=0.0245 and wR_2=0.0584 in $Ca_3Nd_3(BO_3)_5$ for all reflections, respectively. Detailed crystallographic data and refinements for $Cd_4NdO(BO_3)_3$ and $Ca_3Nd_3(BO_3)_5$ are listed in table 1. Atomic coordinates and equivalent isotropic temperature factors are listed in tables 2 and 3.

Table 1. The crystallographic data and refinement conditions for $Cd_4NdO(BO_3)_3$ and $Ca_3Nd_3(BO_3)_5$.

Chemical formula	$Cd_4NdO(BO_3)_3$	$Ca_3Nd_3(BO_3)_5$
Formula weight (g/mol)	786.27	847.01
Temperature (K)	301	296
Crystal system	monoclinic	hexagonal
Space group	*C*m	*P*6$_3$mc
a (Å)	8.0536(14)	10.4864(2)
b (Å)	15.872(2)	10.4864(2)
c (Å)	3.5364(6)	6.2665(1)
α (°)	90	90
β (°)	100.268(7)	90
γ (°)	90	120
Vol ($Å^3$)	444.82(13)	596.772(12)
Z	2	2
Crystal size (mm^3)	0.12×0.07×0.04	0.13×0.11×0.10
μ (cm^{-1})	15.182	14.24
Radiation (MoKα)	0.71073	0.71073
Range for data collection (°)	2.566-27.682	2.24-27.47
Index ranges	-10< h<10, -20< k<20, -4< l<4	-10< h<11, -12< k<12, -8< l<6
Reflections measured	2349	3478
Goodness of fit S	1.084	1.191
Flack parameter	0.15(5)	0.02(2)
Final R_1,wR_2 (I > 2σ(I))	0.0311/0.0730	0.0245/0.0584
R_1, wR_2 (all data)	0.0320/0.0745	0.0245/0.0584
Largest diff peak and hole (e/$Å^3$)	1.26, -1.65	0.83, -1.56

Table 2. Atomic coordinates and equivalent isotropic temperature factors of $Cd_4NdO(BO_3)_3$.

Atom	Wyck.	x/a	y/b	z/c	U[$Å^2$]
Nd1	2a	0.00629(17)	0	0.0063(3)	0.0195(4)
Cd1	4b	0.85541(13)	0.61244(7)	0.6642(2)	0.0112(4)
Cd2	4b	0.73615(16)	0.82197(7)	0.3562(3)	0.0137(4)
O1	4b	0.5378(16)	0.9240(8)	0.234(3)	0.014(2)
O2	2a	0.682(2)	1/2	0.583(5)	0.018(4)
O3	4b	1.028(2)	0.7281(9)	0.704(4)	0.027(3)
O4	4b	0.9051(16)	0.8539(9)	-0.089(4)	0.020(3)
O5	4b	0.704(2)	0.6771(9)	1.110(4)	0.028(3)
O6	2a	-0.208(2)	0	0.405(5)	0.021(4)
B1	4b	0.549(2)	0.6984(12)	0.912(5)	0.010(3)
B2	2a	0.622(3)	1.0000	0.298(8)	0.011(5)

Table 3. Atomic coordinates and equivalent isotropic temperature factors of $Ca_3Nd_3(BO_3)_5$.

Atom	Wyck.	*x/a*	*y/b*	*z/c*	U[Å^2]
Nd1	6c	0.84512(2)	0.15488(2)	0.50028(16)	0.0090(2)
Ca1	6c	0.52716(8)	0.05432(16)	0.1802(3)	0.0039(4)
O1	6c	0.7740(3)	0.2260(3)	0.1663(9)	0.0094(12)
O2	6c	0.5895(3)	0.1789(7)	0.5189(14)	0.0138(13)
O3	12d	0.2994(5)	-0.0691(4)	0.3629(9)	0.0088(9)
O4	6c	0.9240(2)	0.0760(2)	0.1571(10)	0.0117(13)
B1	2b	2/3	1/3	0.525(3)	0.011(3)
B2	6c	0.8037(6)	0.1963(6)	-0.0330(16)	0.0063(18)
B3	2a	1.0000	0	0.157(3)	0.010(3)

Luminescence properties and thermal analysis

The $Cd_4NdO(BO_3)_3$ powders from solid-state synthesis and the $Ca_3Nd_3(BO_3)_5$ powders ground from as-grown single crystals were employed for optical measurements. The room temperature diffuse reflectance spectra of polycrystalline samples were performed on a Cary 5000 UV-visible-NIR spectrophotometer in the wavelength range of 200-1000 nm. The fluorescence and lifetime spectra were recorded on an Edinburgh Instruments FLS980 fluorescence spectrometer with a scan step width of 1 nm and a dwell time of 0.2 s/step in the wavelength range of 800-1400 nm using Xe lamp as light source. The differential scanning calorimetry and thermo-gravimetric analysis (DSC-TG) were carried out with a NETZSCH STA 449C thermal analyzer. The samples were put in alumina crucibles and heated to 1200 ^{o}C with a heating rate of 10 ^{o}C/min in a nitrogen atmosphere and then cooled down to room temperature at a rate of 10 ^{o}C/min.

Second-harmonic generation

For the powder second harmonic generation (SHG) test, a Nd^{3+}:YAG laser of wavelength 1064 nm was adopted as incident light and the KDP powders are utilized as references. Since the powder SHG efficiency based on the Kurtz-Perry method depends strongly on particle size [15], the title crystals and the references were both ground and sieved into five distinct size ranges: 50-61, 61-100, 100-150, 150-300, and 300-450 μm.

Results and Discussion

Phase analysis and thermal stability

As shown in Fig.1 the XRD pattern of $Cd_4NdO(BO_3)_3$ synthesized at 900 ^{o}C is consistent with the simulated pattern. The sample was further heated to 1000 ^{o}C and held at this temperature for 10 h and powder XRD showed that the sample was stable even though it seemed to be partly melted, which was in good agreement with its DSC curve (Fig.S1). In the DSC-TG curves, there is an endothermic peak in the range of 980-1060 ^{o}C and it can be concluded that $Cd_4NdO(BO_3)_3$ is a congruent melting compound and its melting point is about 1020 ^{o}C. $Ca_3Nd_3(BO_3)_5$ crystal decomposed to mainly $NdBO_3$ and other unknown compounds after annealing at 750 ^{o}C for 10 h (see Fig.2), which was confirmed by its DSC curve (Fig.S2). In the DSC curve, a sharp endothermic peak around 730 ^{o}C is observed and it can be certified as its decomposition point.

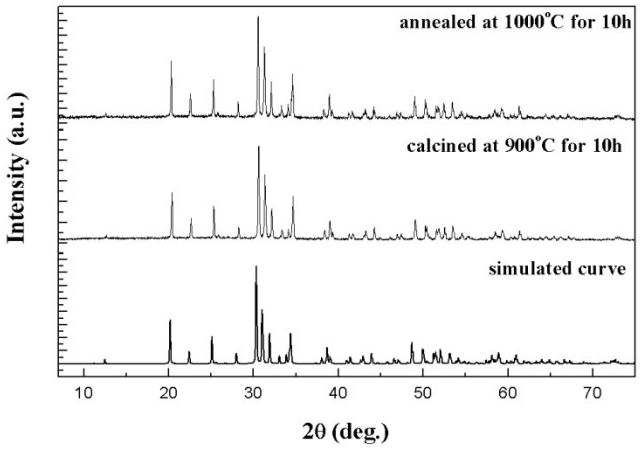

Figure 1. XRD pattern for $Cd_4NdO(BO_3)_3$ under different heat treatment conditions.

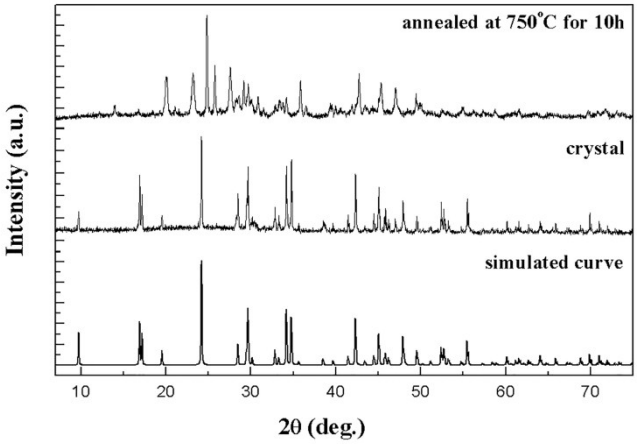

Figure 2. XRD pattern for $Ca_3Nd_3(BO_3)_5$.

Crystal structures

$Cd_4NdO(BO_3)_3$ crystallizes in the monoclinic space group of *C*m which is isostructural with its derivatives $Cd_4ReO(BO_3)_3$ (Re=Y, Gd, Lu). It displays an intricate three-dimensional framework composed by the connection of $Cd1O_6$, $Cd2O_5$ and $Nd1O_6$ distorted polyhedra and BO_3 planar triangles (Fig.3). In the structure, the B atoms have two types of planar BO_3 groups with B-O bond lengths ranging from 1.342(24) to 1.416(13) Å. All $B1O_3$ planar triangles are arranged approximately parallel to the (001) plane, while $B2O_3$ groups are tilted to $B1O_3$ triangles. Two Cd atoms coordinate to O atoms to form $Cd1O_6$ and $Cd2O_5$ distorted polyhedra, respectively. The Cd-O bond lengths in $Cd1O_6$ and $Cd2O_5$ range from 2.248(8) to 2.384(9) Å and from 2.235(10) to 2.458(10) Å, respectively. The Nd atom occupies an unequal 2*a* site and is surrounded by 6 oxygen to form NdO_6 distorted octahedron with Nd-O bond lengths ranging from 2.237(12) to 2.491(13) Å. The NdO_6 octahedron construct chains along the c axis via sharing edge, and CdO_n (n = 5, 6) polyhedra join those chains together to form a 3-dimensional network.

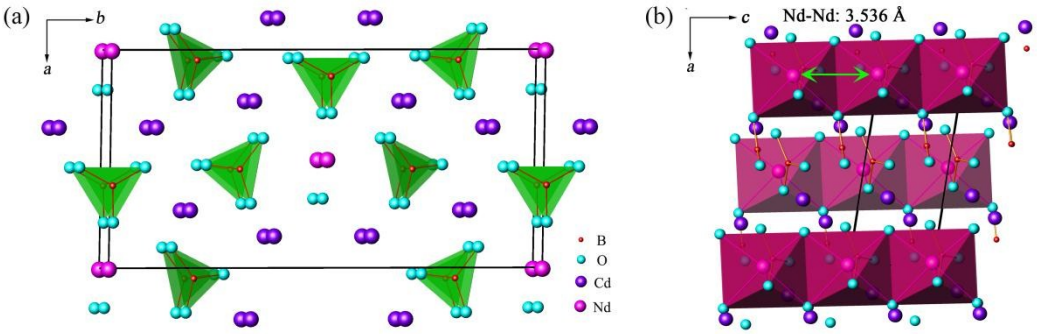

Figure 3. Structure of $Cd_4NdO(BO_3)_3$ crystal: (a) viewing from the [001] direction, (b) and the arrangement of NdO_6 octahedron in the ac plane.

$Ca_3Nd_3(BO_3)_5$ has a hexagonal cell with lattice parameters a = 10.4864 (2) Å and c = 6.2665(1) Å and it belongs to space group $P6_3mc$, which is isostructural to $Ca_3La_3(BO_3)_5$. There are three types of BO_3 triangles with B-O bondlengths ranging from 1.360(12) to 1.403(6) Å. The Ca^{2+} ion is surrounding by eight O atoms to form CaO_8 distorted polyhedron (Ca-O bond lengths: 2.300(2)-2.647(5) Å) and the Nd atom coordinates to 10 O atoms forming NdO_{10} polyhedron (Nd-O bond lengths: 2.452(4)-2.8180(7) Å). In the structure three NdO_{10} polyhedra link together to enclose one BO_3 triangle to form a $[Nd_3O_{24}(BO_3)]$ cluster (see Fig.4b). The clusters extend in the *ab* plane developing into a layer of Kagomé lattice [16] with triangular Nd-Nd interaction and the layers are further connected in the c direction by sharing the edges of NdO_{10} polyhedra.

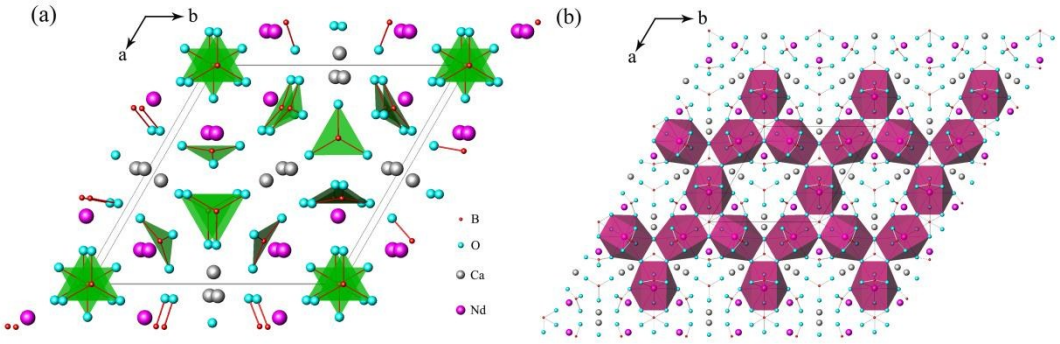

Figure 4. Structure of $Ca_3Nd_3(BO_3)_5$ crystal: (a) viewing from the [001] direction, (b) and a layer of Kagomé lattice composed of NdO_{10} polyhedra in the ab plane.

According to the structural parameters, it can be calculated that the Nd^{3+} concentrations of the two compounds are 4.5×10^{21} ions/cm^3 in $Cd_4NdO(BO_3)_3$ and 1.0×10^{22} ions/cm^3 in $Ca_3Nd_3(BO_3)_5$ respectively, which are at the same level as the Nd^{3+} concentrations in NAB crystal. From the crystal structure results, although $Ca_3Nd_3(BO_3)_5$ has a higher Nd^{3+} concentrations, its distance between the nearest Nd^{3+} ions (4.211 Å) is longer than that in $Cd_4NdO(BO_3)_3$ (3.536 Å), which indicates that the Nd^{3+} ions are more uniformly distributed in $Ca_3Nd_3(BO_3)_5$ crystal lattice. It is reported that long fluorescence lifetime at high doping levels can be expected if the dopants are far apart [7]. Therefore, $Ca_3Nd_3(BO_3)_5$ may have a longer decay time of $^4F_{3/2}$ to $^4I_{11/2}$ transition than $Cd_4NdO(BO_3)_3$.

Diffuse reflectance spectrum

The UV-visible-NIR diffuse reflectance spectra of the two compounds are shown in Fig. 5, which show typical spectra [17] of Nd^{3+} optical intense absorptions. Six main absorption bands with wavelength range from 300 to 900nm can be found in $Cd_4NdO(BO_3)_3$ spectrum, which are centered at about 355, 532, 590, 738, 795 and 873 nm respectively. Similar peaks centered about 355, 470, 524, 582, 681, 742, 798, and 873 nm were also observed in $Ca_3Nd_3(BO_3)_5$. All these peaks can be assigned to the Nd^{3+} transitions in the 4f electronic shell from ground state $^4I_{9/2}$ to other excited levels, such as $^4F_{3/2}$ - $^4F_{9/2}$ (900 - 650 nm), $^4G_{5/2}$ - $^2G_{11/2}$ (600 - 450 nm), and $^4D_{5/2}$ - $^4D_{1/2}$ (~ 355 nm) [18]. It is worth noting that the absorptions at about 800 nm arising from the transition of $^4I_{9/2}$ to $^4F_{5/2}$ in both two compounds are broad, a favorable feature for laser diode pumping in microchip application.

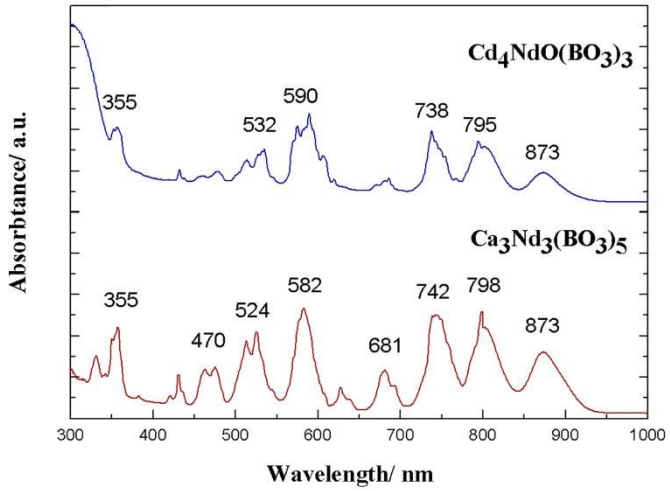

Figure 5. The diffuse reflectance spectrum of $Cd_4NdO(BO_3)_3$ and $Ca_3Nd_3(BO_3)_5$ polycrystalline powders.

Luminescent properties

The emission spectrum of $Cd_4NdO(BO_3)_3$ and $Ca_3Nd_3(BO_3)_5$ excited at 320 and 355 nm, were presented in Fig.6. Main broad emissions around 1060 nm are observed for both compounds, which can be attribute to the Nd^{3+} emission of $^4F_{3/2}$ to $^4I_{11/2}$. These emission bands are split into two strong peaks at 1061 nm and 1068 nm in $Cd_4NdO(BO_3)_3$ and 1059 nm and 1070 nm in $Ca_3Nd_3(BO_3)_5$ respectively, caused by the splitting of the $^4I_{11/2}$ state in the crystal field. As usual, two more emission bands are observed near 900 nm and 1330 nm, which can be attribute to the Nd^{3+} ion transition from $^4F_{3/2}$ to $^4I_{9/2}$ and from $^4F_{3/2}$ to $^4I_{13/2}$, respectively.

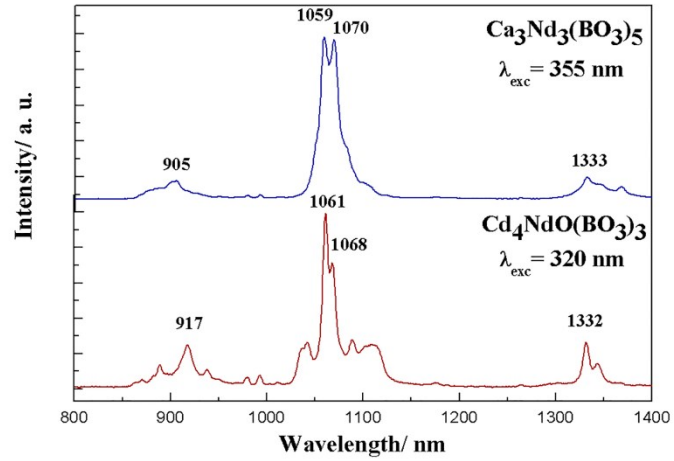

Figure 6. The emission spectrum of polycrystalline samples of $Cd_4NdO(BO_3)_3$ and $Ca_3Nd_3(BO_3)_5$ polycrystalline powders.

The fluorescence decay curve of $Cd_4NdO(BO_3)_3$ and $Ca_3Nd_3(BO_3)_5$ was measured and its lifetime was fitted to be 7.19 μs and 42.97 μs (Fig.7). The shorter decay time of $Cd_4NdO(BO_3)_3$ comparing to $Ca_3Nd_3(BO_3)_5$ may result from its shorter distance between the nearest Nd^{3+} ions and stronger interaction between the neighboring Nd-O polyhedra. Because of its high Nd^{3+} concentration and longer fluorescence lifetime, $Ca_3Nd_3(BO_3)_5$ might be a better candidate for self-activated microchip laser media comparing with $Cd_4NdO(BO_3)_3$.

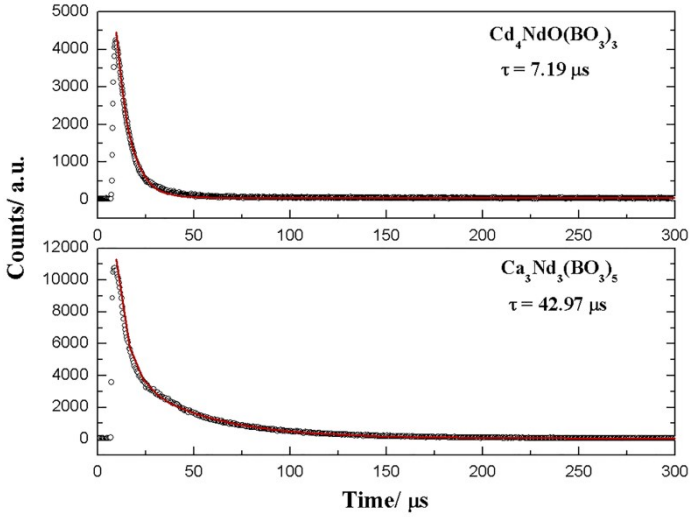

Figure 7. The fluorescence decay time of the $^4F_{3/2}$-$^4I_{11/2}$ transition in $Cd_4NdO(BO_3)_3$ and $Ca_3Nd_3(BO_3)_5$.

Non-linear optical property

The SHG signals are found to be about 0.7 ×KDP and 0.5 ×KDP for $Cd_4NdO(BO_3)_3$ and $Ca_3Nd_3(BO_3)_5$, respectively. The results cannot be decisive because the Nd^{3+} ions absorbs SHG signal at 532 nm [19], which can also been seen in the absorption spectra (Fig.5). Nonetheless, isostructural compounds $Cd_4ReO(BO_3)_3$ were found to have large NLO coefficients (5 ×KDP) arising from aligned BO_3 groups [20, 21] and CdO_n groups with a polar displacement of the d^{10} Cd^{2+} cation [13, 22, 23]. Thus $Cd_4NdO(BO_3)_3$ might have more advantage on the application as self-frequency-doubling (SFD) laser crystal like a number of Nd^{3+}-doped borates, such as Nd^{3+}:$YAl_3(BO_3)_4$ (NYAB) [24], Nd^{3+}:$GdAl_3(BO_3)_4$ (NGAB) [25], Nd^{3+}: $YCa_4O(BO_3)_3$ (Nd:YCOB) [26].

Conclusion

Two orthoborates of $Cd_4NdO(BO_3)_3$ and $Ca_3Nd_3(BO_3)_5$ have been grown by the flux method. The structure of the former crystal displays an three-dimensional framework composed by the connection of $Cd1O_6$, $Cd2O_5$ and $Nd1O_6$ distorted polyhedra and BO_3 planar triangles, while the latter consists of $[Nd_3O_{24}(BO_3)]$ layers of Kagomé lattice interconnected by edge sharing NdO_{10} polyhedral and BO_3 triangles. Similar to the well-known self-activated crystal NAB, the two compounds both have high Nd^{3+} concentration with 4.5×10^{21} ions/cm^3 in $Cd_4NdO(BO_3)_3$ and 1.0×10^{22} ions/cm^3 in $Ca_3Nd_3(BO_3)_5$. They both have strong emission peaks around 1060 nm related to the transition of $^4F_{3/2}$ to $^4I_{11/2}$ in their fluorescence spectrum. The fluorescence lifetime of $Ca_3Nd_3(BO_3)_5$ is fitted to be 42.97 μs, which is longer than that of NAB crystal. Therefore, it is concluded that $Ca_3Nd_3(BO_3)_5$ may be a promising potential candidate crystal as NAB for self-activated microchip laser media. Though the fluorescence lifetime of $Cd_4NdO(BO_3)_3$ is much shorter (7.19 μs), the large SHG response of this crystal may find application as self-frequency doubling material.

Acknowledgments

This work is financially supported by the National Natural Science Foundation of China (Grant No. 90922036 and No. 51502307) and National Instrumentation Program (No. 2012YQ120048).

Notes and References

[a] *Beijing Center for Crystal Research and Development, Technical Institute of Physics and Chemistry, Chinese Academy of Sciences, Beijing 100190, P. R. China. Tel.:0086-010-82543711; E-mail: rkli@mail.ipc.ac.cn.*
[b] *Graduate University of Chinese Academy of Sciences, Beijing 100049, P. R. China*

†Electronic Supplementary Information (ESI) available: The crystallographic data for $Cd_4NdO(BO_3)_3$ and $Ca_3Nd_3(BO_3)_5$ has been deposited to CCDC. CCDC number is 1429008 for $Cd_4NdO(BO_3)_3$ and 1429009 for $Ca_3Nd_3(BO_3)_5$. Electronic files of the crystal structure data (CIF).

1 J. J. Zayhowski, *Optical Materials*, 1999, **11**, 255-267.
2 J. Li, J. Y. Wang, Y. Zhang, T. Z. Zhang, *J. Cryst. Growth*, 2013, **381**, 61.
3 F. X. Shan, M. J. Xia, G. C. Zhang, J. Y. Yao, X. Y. Zhang, T. X. Xu, Y. C. Wu, *Solid State Sciences*, 2015, **41**, 31-35.
4 H. Y. P. Hong, K. Dwight, Mater. Res. Bull., 1974, **9**, 1661.
5 M. Montes, D. Jaque, Z. D. Luo, Y. D. Huang, *Opt. Lett.*, 2005, **30**, 397.
6 F. Gan, *Laser Materials*, World Scientif ic, Singapore, 1994.
7 H.Y.P. Hong, K. Dwight, Mater. Res. Bull., 1974, **9**, 775-780.
8 H.Y.P. Hong, *Acta Crystallogr. Sect. B*, 1974, **30**, 468.
9 D. Jaque, O. Enguita, J. Garc´ıa Sol`e, A. D. Jiang, and Z. D. Luo, *Appl. Phys. Lett.*, 2000, **76**, 2176.
10 N. I. Leonyuk, E. V. Koporulina, V. V. Maltsev, A. V. Mokhov, O. V. Pilipenko, *J. Cryst. Growth*, 2005, **281**, 587.
11 Y. Zhang, J. K. Liang, X. L. Chen, M. He, T. Xu, *Journal of Alloys and Compounds*, 2001, **327**, 96-99.
12 T. Y. Zhou and N. Ye, *Acta Cryst*., 2008. **E64**, i37.
13 G. H. Zou, Z. J. Ma, K. C. Wu and N. Ye, *J. Mater. Chem.*, 2012, **22**, 19911-19918.
14 G. M. Sheldrick, *Acta Crystallogr.*, 2008, **A 64**, 112-122.
15 S. K. Kurtz, T. T. Perry, *J. Appl. Phys.*, 1968, **39**, 3798-3813.
16 R. K. Li and C. Greaves, *Physical Review B*, 2003, **68**, 172403.
17 J. B. Gruber, D. K. Sardar, T. H. Allik, B. Zandi, *Optical Materials*, 2004, **27**, 351-358.
18 W. T. Carnall, P. R. Fields, K. Rajnak, *J. Chem. Phys.*, 1968, **49**, 4424.
19 W. Zhao, W. W. Zhou, M. J. Song, G. F. Wang, J. M. Du, H. J. Yu, J. X. Chen, *Optical Materials*, 2011, **33**, 647-654.
20 C. T. Chen, Y. C. Wu, R. K. Li, *Int. Rev. Phys. Chem.*, 1989, **8**, 65-91.
21 C. T. Chen, Y. C. Wu, R. K. Li, *J. Cryst. Growth*, 1990, **99**, 790-798.
22 W. L. Zhang, W. D. Cheng, H. Zhang, L. Geng, C. S. Lin and Z. Z. He, *J. Am. Chem. Soc.*, 2010, **132**, 1508.
23 Y. Inaguma, M. Yoshida and T. Katsumata, *J. Am. Chem. Soc.*, 2008, **130**, 6704.
24 L. M. Dorozhkin, I. I. Kuratev, N. I. Leonyuk, T. I. Timchenko, and A. V. Shestakov, *Sov. Tech. Phys. Lett.*, 1981, **7**, 555.
25 C. Y. Tu, M. W. Qiu, Y. C. Huang, X. Y. Chen, A. D. Jiang, and Z. D. Luo, *J. Cryst. Growth.*, 2000, **208**, 487.
26 B. H. T. Chai, J. M. Eichenholz, Q. Ye, W. K. Jang, L. Shah, G. M. Luntz, and M. Richardson, in: W. R. Bosenberg, M. M. Fejer (Eds.), OSA TOPS, *Proc. Adv. Solid St. Lasers*, 1998, **19**, 56.

Graphical abstract

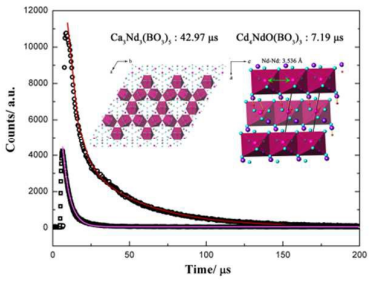

Different arrangements of NdO_n polyhedra in the two crystal structures can result in huge difference of their fluorescence lifetime.